NRL Memorandum Report 6391

Three Dimensional Cloud Dynamics: Preliminary Application to a HANE Environment

J. D. HUBA, J. F. DRAKE* AND M. MULBRANDON

Geophsical and Plasma Dynamics Branch
Plasma Physics Division

**Science Applications International Corporation*
McLean, VA 22102

January 30, 1989

This research was supported by DNA under Project/Task Code and Title: RB RC/Atmospheric Effects and Mitigation, Work Unit Code and Title: 00166/Plasma Structure Evolution.

SECURITY CLASSIFICATION OF THIS PAGE

REPORT DOCUMENTATION PAGE

Form Approved
OMB No 0704-0188

1a REPORT SECURITY CLASSIFICATION UNCLASSIFIED	1b RESTRICTIVE MARKINGS
2a SECURITY CLASSIFICATION AUTHORITY	3 DISTRIBUTION / AVAILABILITY OF REPORT Approved for public release; distribution unlimited.
2b DECLASSIFICATION / DOWNGRADING SCHEDULE	
4 PERFORMING ORGANIZATION REPORT NUMBER(S) NRL Memorandum Report 6391	5 MONITORING ORGANIZATION REPORT NUMBER(S)
6a NAME OF PERFORMING ORGANIZATION Naval Research Laboratory 6b OFFICE SYMBOL (If applicable) Code 4780	7a NAME OF MONITORING ORGANIZATION
6c ADDRESS (City, State, and ZIP Code) Washington, DC 20375-5000	7b ADDRESS (City, State, and ZIP Code)
8a NAME OF FUNDING / SPONSORING ORGANIZATION Defense Nuclear Agency 8b OFFICE SYMBOL (If applicable) RAAE	9 PROCUREMENT INSTRUMENT IDENTIFICATION NUMBER
8c ADDRESS (City, State, and ZIP Code) Washington, DC 20305	10 SOURCE OF FUNDING NUMBERS PROGRAM ELEMENT NO: MIPR 88-526 PROJECT NO: RB RC TASK NO: 00166 WORK UNIT ACCESSION NO
11 TITLE (Include Security Classification) Three Dimensional Cloud Dynamics: Preliminary Application to a HANE Environment	
12 PERSONAL AUTHOR(S) Huba, J.D., Drake,* J.F. and Mulbrandon, M.	
13a TYPE OF REPORT Interim 13b TIME COVERED FROM _____ TO _____ 14 DATE OF REPORT (Year, Month, Day) 1989 January 30 15 PAGE COUNT 32	
16 SUPPLEMENTARY NOTATION *Science Applications International Corporation, McLean, VA 22102. (Continues)	
17 COSATI CODES FIELD / GROUP / SUB-GROUP	18 SUBJECT TERMS (Continue on reverse if necessary and identify by block number)

19 ABSTRACT (Continue on reverse if necessary and identify by block number)

The 3D plasma cloud dynamics model of Drake et al. (1988) is applied to barium clouds and to nuclear striations. Quantitative estimates of the critical scale size for marginal stability are presented. The implications of these results regarding the 'freezing' of plasma striations are discussed.

20 DISTRIBUTION / AVAILABILITY OF ABSTRACT ☒ UNCLASSIFIED/UNLIMITED ☐ SAME AS RPT ☐ DTIC USERS	21 ABSTRACT SECURITY CLASSIFICATION UNCLASSIFIED
22a NAME OF RESPONSIBLE INDIVIDUAL J.D. Huba	22b TELEPHONE (Include Area Code) (202) 767-3630 22c OFFICE SYMBOL Code 4780

DD Form 1473, JUN 86 *Previous editions are obsolete* SECURITY CLASSIFICATION OF THIS PAGE

S/N 0102-LF-014-6603

SECURITY CLASSIFICATION OF THIS PAGE

16. SUPPLEMENTARY NOTATION (Continued)

This research was supported by DNA under Project/Task Code and Title: RB RC/ Atmospheric Effects and Mitigation, Work Unit Code and Title: 00166/Plasma Structure Evolution.

DD Form 1473, JUN 86 (Reverse)

CONTENTS

THREE DIMENSIONAL CLOUD DYNAMICS: PRELIMINARY APPLICATION TO A HANE ENVIRONMENT

I. INTRODUCTION

The Defense Nuclear Agency is sponsoring a broad-based research program on the dynamics and phenomenology of high altitude nuclear explosions (HANEs). An important goal of this research is to understand and model the late time nuclear environment; specifically, the intense field-aligned striations which are produced. These striations are regions of high electron density and are of military significance because they can adversely impact communication and surveillance systems. Of particular interest to DNA is the development of a model which characterizes the power spectral density of nuclear striations: the outer scale, the freezing scale, the inner scale, and the associated power law exponents between these scale sizes. This information provides a description of the late time nuclear environment which can be used in propagation codes relevant to military systems.

See #1473

It is generally believed that the outer scale is related to the macroscopic size of the striations (or clumps of striations), while the inner scale is related to dissipative effects (i.e., diffusion). The freezing scale length is associated with plasma dynamics at scale sizes between the inner and outer scale length and is associated with a 'break' in the power law exponent. This type of power spectral density is observed in naturally occurring structured ionospheric environments (e.g., equatorial spread F, high latitude blobs). Since it is believed that the fundamental structuring processes are the same in both the ambient and HANE environments, then it is expected that the power spectral densities will be similar, at least qualitatively.

Recently, DNA researchers have focussed on developing a model for the freezing scale length (k_f^{-1}) which can be implemented in conjunction with the DNA code SCENARIO. One freezing model that has been developed is the

Manuscript approved July 14, 1988.

JAYCOR freezing model (Sperling et al., 1988). This model attributes the freezing scale length to collisional viscosity and/or magnetic viscosity depending on the ionospheric parameters. This model emphasizes the dynamics of the plasma transverse to the magnetic field and incorporates parallel effects in a qualitative manner. In contrast to this model, recent studies at NRL (Drake and Huba, 1986; 1987; Drake et al., 1988) have shown that parallel dynamics (i.e., 3D effects) can play the key role in the 'freezing' of plasma clouds (or striations). In particular, a stability criterion has been derived which indicates that plasma clouds (or striations) are stable against large-scale structuring when $r_c > r_{cr}$; here r_c is the radius of the cloud transverse to $\underset{\sim}{B}$, and r_{cr} is a 'critical' radius which is a function of the physical parameters of the system. The purpose of this report is to present quantitative estimates of r_{cr} for parameters typical of barium clouds and nuclear striations based upon the NRL 3D model and to discuss the implications of these results regarding the freezing scale length.

For the case of barium clouds, we find the critical scale size for marginal stability is $r_{cr} \lesssim 100$ m, i.e., barium clouds with $r_c > r_{cr}$ are stable. Since the scale size of 'frozen' barium clouds is ~ 100's m, we conclude that our theoretical results are consistent with the observations: 3D effects can provide the physical mechanism to 'freeze' barium clouds at the observed scale sizes. Although this result is very significant, it does not explain the actual scale size of the striations. We suggest the following hypothesis regarding the structuring of barium clouds. During the initial phase of a barium cloud expansion, the cloud evolves dynamically. The cloud diffuses along the magnetic field, and in the presence of a neutral wind or ambient electric field it steepens on one side. Eventually, the steepened 'backside' of the cloud can become

unstable to the $\underset{\sim}{E} \times \underset{\sim}{B}$ instability and the cloud structures. During this phase, the waterbag cloud model used in our 3D theory is not appropriate, and hence, our theory is not applicable. This is not to say that 3D effects are not important during the onset of instability, but only that the quantitative analysis in Drake et al. (1988) is not valid. Subsequent to the initial break-up of the cloud, the smaller clouds (or fingers) may evolve into waterbag-like equilibria. If this is the case, then we can apply the NRL 3D model and ask the question: Are these smaller clouds stable or unstable? If they are stable, as our analysis indicates, then 3D effects can account for 'freezing'. As to the distribution of frozen scale sizes, this would be determined by the initial break-up of the cloud.

Applying our model to plasma parameters believed typical of nuclear striations, we find that the critical scale size is in the range $r_{cr} \simeq$ 10's m - 100's km. The reason for this rather broad range of values is due to the broad parameter regime considered. Thus, unlike the situation for barium clouds, it is not clear that the initial set of nuclear striations will be stable to further structuring because of 3D effects. Nevertheless, early time structuring ($t \lesssim$ few min) will probably play an important role in setting up a distribution of striation scale sizes which may affect late time phenomenology, and hence should be more thoroughly investigated.

II. CRITICAL RADIUS MODEL

The plasma and field configuration used in Drake et al. (1988) is described as follows. The magnetic field is in the z-direction ($\underset{\sim}{B} = B \hat{e}_z$), the neutral wind is in the x-direction ($\underset{\sim}{V}_n = V_n \hat{e}_x$), and a waterbag model is assumed for the density, i.e., $n_0 = n_c + n_b$ inside the cloud and $n_0 = n_b$ outside the cloud where the subscripts c and b denote cloud and background,

respectively. The cloud is assumed to be circular in the plane transverse to $\underset{\sim}{B}$ and is an arbitrary ellipse in the plane containing $\underset{\sim}{B}$.

The equilibrium potential for this configuration consists of two components: a polarization potential caused by the neutral wind, and an ambipolar potential caused by electron pressure parallel to $\underset{\sim}{B}$. The polarization potential causes the cloud to move in the direction of the neutral wind (albeit at a reduced speed). The relative ion-neutral slip velocity is the driving mechanism for the gradient drift instability which can cause the cloud to structure. The ambipolar potential causes the cloud to spin about the axis aligned with the magnetic field. The rotation rate varies with position along the length of the cloud (i.e., along $\underset{\sim}{B}$), so that there is a 'shear' in the cloud velocity in this direction.

A stability analysis was performed based upon this equilibrium and a stability criterion was derived [Drake et al., 1988]. The marginal stability criterion for the cloud is given by

$$\Gamma = \Gamma_c \tag{1}$$

where

$$\Gamma = \frac{c(T_e + T_i)}{eB} \frac{1}{V_n} \frac{1}{r_c} \tag{2}$$

$$\Gamma_c = z_c^2 \left(1 - \frac{V_0}{V_n}\right) \cos\phi_0 \tag{3}$$

where ϕ_0 is determined from

$$\omega_0\left(\phi_0,\ \Gamma_c,\ M,\ z_c\right) = 0 \tag{4}$$

These expressions are (52a) and (52b) in Drake et al. (1988). Here, r_c is the radius of the cloud, $z_c = (L_z/r_c)(\sigma_\perp/\sigma_{||})^{1/2}$, L_z is the half-length of the cloud along $\underset{\sim}{B}$, $\sigma_{||,\perp}$ are the parallel and perpendicular conductivities, respectively, [$\sigma_{||}/\sigma_\perp = (\Omega_e\Omega_i/\nu_e\nu_i)^{1/2}$ where Ω_α is the cyclotron frequency of species α, $\nu_e = \nu_{ei} + \nu_{en}$ and $\nu_{\alpha\beta}$ is the collision frequency between species α and β], $M = n_c/n_b$, ϕ_0 is the azimuthal angle for mode localization, V_0 is the cloud speed, and ω_0 is the azimuthal mode frequency. Clouds are stable for $\Gamma > \Gamma_c$ and are unstable for $\Gamma < \Gamma_c$.

This stability criterion is based upon two distinct physical effects: convection and shear. First, the condition $\omega_0 = 0$ requires the mode to be non-propagating; this results from a balance of the diamagnetic propagation of the mode, and the azimuthal background plasma flow. If this condition cannot be met, then the cloud is stable because perturbations are rapidly convected from the unstable 'backside' of the cloud to the stable 'front-side' of the cloud. This stabilizing mechanism is discussed in detail in Drake and Huba (1986). The second stabilizing mechanism results from shear stabilization. As noted earlier, the azimuthal flows generated by the ambipolar potential are not uniform along the length of the cloud. This sheared flow causes the perturbations to have $k_z \neq 0$ which gives rise to the damping of the mode. This point is discussed in detail in Drake et al. (1988).

The stability criterion can be simplified by considering the limits $z_c \gg 1$, $z_c = 1$, and $z_c \ll 1$ (Drake et al., 1988). We find that (3) can be written as

$$\Gamma_c = \begin{cases} 2z_c^2 \cos\phi_0/(M+2) & z_c \gg 1 \\ 2z_c^2 \cos\phi_0/(M+3) & z_c = 1 \\ (2/\pi)z_c^2 \cos\phi_0/(2/\pi + Mz_c) & z_c \ll 1 \end{cases} \qquad (5)$$

We further simplify (5) by taking $\phi_0 \sim 0°$ for $z_c < 1$ and $\phi_0 \sim 45°$ for $z_c \geq 1$. This approximation is based upon exact solutions to (1) - (4), and is used in order to develop a simple model for the critical cloud radius. We obtain the following marginal stability condition

$$\Gamma = \Gamma_c \equiv \begin{cases} \sqrt{2}\, z_c^2/(M+2) & z_c \gg 1 \\ 3\sqrt{2}\, z_c^2/2(M+3) & z_c = 1 \\ (2/\pi) z_c^2/(2/\pi + M z_c) & z_c \ll 1 \end{cases} \tag{6}$$

However, we note that our goal is to determine a critical striation radius, r_{cr}, based upon (6). In order to do this we proceed in the following manner. We define Γ_0 as follows

$$\Gamma_0 = \frac{c\left(T_e + T_i\right)}{eB} \frac{1}{V_n} \frac{1}{L_z} \left(\frac{\sigma_{||}}{\sigma_\perp}\right)^{1/2} \tag{7}$$

so that

$$\Gamma = \Gamma_0 z_c. \tag{8}$$

Substituting (8) into the marginal stability condition (6) we arrive at a new marginal stability condition

$$\Gamma_0 = \Gamma_{c0} \equiv \begin{cases} \sqrt{2}\, z_c/(M+2) & z_c \gg 1 \\ 3\sqrt{2}\, z_c/2(M+3) & z_c = 1 \\ (2/\pi) z_c/(2/\pi + M z_c) & z_c \ll 1 \end{cases} \tag{9}$$

The advantage of using (9) instead of (6) is that Γ_0 does not depend on the transverse radius of the cloud (or striation).

Based upon (9) we determine the critical radius, r_{cr}, as follows. First, we plot Γ_{c0} vs. z_c for a specific value of M. This is shown in Fig. 1 for M = 5.0; note that Γ_{c0} increases monotonically with increasing z_c. In calculating Γ_{c0} we use (9) for $z_c > 10$, $z_c = 1$, and $z_c < 0.1$. The values of Γ_{c0} between $z_c = 0.1$ and 1.0, and $z_c = 1.0$ and 10.0 are calculated assuming linear interpolation between these points. We find this to be a reasonable approximation based upon comparisons with exact solutions of Γ_{c0} using the formulas in Drake et al. (1988). Second, we calculate the value of Γ_0 and plot it as a straight line. For illustrative purposes we assume $\Gamma_0 = 0.5$ in Fig. 1. The marginal stability condition is determined by $\Gamma_0 = \Gamma_{c0}$. Clouds are stable for $\Gamma_0 > \Gamma_{c0}$ and unstable for $\Gamma_0 < \Gamma_{c0}$. This means that clouds are stable for $z_c < z_{cr}$ and unstable for $z_c > z_{cr}$ where $z_{cr} \simeq 2.2$ in Fig. 1. Noting that $z_c = (L_z/r_c)(\sigma_\perp/\sigma_{||})^{1/2}$ we then define the critical radius to be

$$r_{cr} = \frac{L_z}{z_{cr}} \left(\frac{\sigma_\perp}{\sigma_{||}}\right)^{1/2} \tag{10}$$

Thus, clouds are stable for $r_c > r_{cr}$ and are unstable for $r_c < r_{cr}$. The explicit dependence of r_{cr} on the various parameters (e.g., L_z, V_n, $\sigma_{||}/\sigma_\perp$, etc.) is described in the Appendix.

III. QUANTITATIVE RESULTS

We now present a series of figures which plot r_{cr} as a function of different physical parameters representative of barium clouds and nuclear striations.

First, we consider barium clouds. In Fig. 2 we plot r_{cr} (meters) vs. $\sigma_{||}/\sigma_\perp$ for M = 10, $T_e = T_i = 0.1$ eV, B = 0.3 G, $V_n = 100$ m/sec, and $L_z = 5$ km, 10 km, 15 km, 20 km, and 40 km. Barium clouds are observed to structure when $L_z \sim 15 - 30$ km [Linson, 1972]. For clouds at altitudes ~

180 km we estimate $\sigma_{||}/\sigma_{\perp} \sim 6.25 \times 10^4$. From Fig. 2 we see that $r_{cr} \lesssim 10$'s m for $L_z < 40$ km. Thus, barium clouds with transverse scale sizes greater than 10's m are stable to further structuring by the gradient drift instability because of 3D effects. This is consistent with observational evidence which suggests that barium clouds are frozen for $r_c \sim 100$'s m. However, we add that the critical radius determined by our theory does not predict the predominance of cloud striations with $r_c \sim 100$'s m. We discuss this point further in the final section.

We now turn our attention to parameters typical of nuclear striations. In Fig. 3 we plot r_{cr} (km) vs. $\sigma_{||}/\sigma_{\perp}$ for $L_z = 200$ km, $V_n = 10^3$ m/sec, $T_e = T_i = 0.3$ eV, B = 0.3 G, and M = 5.0, 10.0, 20.0, and 100.0. First, we note that in general, r_{cr} decreases as M increases. Second, as in the case of barium clouds, there is a relatively strong dependence of r_{cr} on $\sigma_{||}/\sigma_{\perp}$. For $\sigma_{||}/\sigma_{\perp} \gtrsim 4.0 \times 10^6$ we note that $r_{cr} < 100$'s m for the values of M chosen. However, for more collisional striations (i.e., $\sigma_{||}/\sigma_{\perp} \lesssim 2.0 \times 10^5$), the critical radius for low to moderate M values is $\gtrsim 10$ km, while for high M values is ~ 100's m. And third, note that r_{cr} becomes independent of M for $\sigma_{||}/\sigma_{\perp} < 10^4$ and $M \lesssim 20$; for these parameters we also have $z_{cr} << 1$. This result is consistent with (10).

In Fig. 4 we plot r_{cr} (km) vs. $\sigma_{||}/\sigma_{\perp}$ for M = 10, $V_n = 10^3$ m/sec, $T_e = T_i = 0.3$ eV, B = 0.3 G, and L_z = 100 km, 200 km, 300 km, and 400 km. The values of r_{cr} are similar to those in Fig. 3, ranging from 10's m to 100's km. We note that r_{cr} decreases as L_z decreases as expected. For relatively short striations ($L_z \sim 100$ km), we find that $r_{cr} \lesssim 10$ km while for longer striations ($L_z \sim 400$ km) that $r_{cr} \lesssim 100$'s km.

In Fig. 5 we plot r_{cr} (km) vs. $\sigma_{||}/\sigma_{\perp}$ for M = 10, $T_e = T_i = 0.3$ eV, B = 0.3 G, $L_z = 200$ km, $V_n = 10^3$ m/sec, 6.7×10^2 m/sec, 3.3×10^2 m/sec, and 10^2 m/sec. We note that r_{cr} decreases substantially as V_n decreases from

10^3 m/sec to a nominal ionospheric value of 10^2 m/sec. For conductivity ratios $\sigma_{||}/\sigma_{\perp} \gtrsim 10^5$ we find that $r_{cr} \lesssim 300$ m when $V_n = 10^2$ m/sec; this value of r_{cr} is similar to the barium cloud results.

IV. DISCUSSION

We have developed a relatively simple procedure to determine the critical transverse scale size of an ionospheric plasma cloud or striation based upon the 3D model of Drake et al. (1988). The critical radius is given by (9) where z_{cr} is determined from (8), i.e., $\Gamma_0 = \Gamma_{c0}$. We find the somewhat surprising result that 'thin' clouds are more unstable than 'fat' clouds (all other parameters being equal). That is, clouds are unstable for $r_c < r_{cr}$, while they are stable for $r_c > r_{cr}$. Applying this model to barium clouds released at ~ 180 km we find that $r_{cr} \lesssim 100$ m; this result is consistent with observational evidence of frozen clouds (or fingers) for r_c ~ 100's m [Linson, 1972]. Applying this model to nuclear striations leads to a broad range of r_{cr} because of the variability of the physical parameters of the system. We find that for weakly collisional plumes (i.e., $\sigma_{||}/\sigma_{\perp} \gtrsim 10^6$) that $r_{cr} \lesssim$ few kms, while for strongly collisional plumes (i.e., $\sigma_{||}/\sigma_{\perp} \lesssim 10^5$) that $r_{cr} > 10$ km.

Although these results are interesting, there are two problems which need to be addressed regarding the development of a freezing scale model based on 3D dynamics. The first problem involves the observed size of frozen barium cloud striations (r_c ~ 100's m). This scale size is <u>not</u> described by our 3D model. An explanation for this is the following. During the early stages of barium cloud evolution, the cloud is relatively diffuse and is not well-described by the 3D waterbag model assumed in Drake et al. (1988). The cloud is not in equilibrium and evolves dynamically with its 'backside' developing a steep gradient. The 'backside' eventually becomes unstable and the cloud 'breaks-up' into smaller clouds (or

fingers). We speculate that the observed freezing scale size is determined during the initial structuring of the cloud. The newly formed smaller clouds may have a density profile similar to the waterbag equilibrium discussed in Drake et al. (1988) (or may evolve into such a profile), and thus, would be stable to further structuring because of 3D effects.

Applying this reasoning to nuclear striations suggests that it is crucial to understand and model the initial onset of structure in the nuclear environment in order to determine the physical scale sizes of striations. However, unlike the barium cloud case, it is not clear that the initial set of scale sizes will be stable to further structuring because of 3D effects. This is because the broad range of physical parameters (e.g., $\sigma_{||}/\sigma_{\perp}$, L_z, V_n, etc.) in a nuclear environment leads to a broad range of critical scale sizes r_{cr}; as shown in Section III, $r_{cr} \simeq$ 10's m - 100's km. It is likely that there will be striations formed with $r_c < r_{cr}$ so that further structuring can occur. Nevertheless, early time structuring (t ~ few min) will probably play an important role in setting up a distribution of striation scale sizes which may persist into late time, and hence should be more thoroughly investigated.

For example, the field-aligned striations which formed during the Checkmate event had transverse scale sizes in the range 300 - 1800 m, most of them were in the range 500 - 700 m (Chesnut, private communication). These striations were produced within a few minutes after the burst. To estimate r_{cr} for Checkmate, we consider an aluminium plasma with $n \simeq 10^8$ cm^{-3}, $T_e = T_i \simeq .3$ ev, $B = 0.3$ G, and $\nu_{in} \simeq 1$ sec^{-1}. For these parameters we find that $\sigma_{||}/\sigma_{\perp} \simeq 2 \times 10^4$. From Fig. 3 we note that $r_{cr} \simeq 2$ km (for $M = 100$, $V_n = 10^3$ m/sec, and $L_z = 200$ km) which is larger than the observed striation radii. However, if we were to take M somewhat larger and V_n

somewhat smaller (e.g., M = 200 and V_n = 400 m/sec) we find that r_{cr} = 300 m. For these parameters, the Checkmate striations would be stable to further structuring by the $\underset{\sim}{E} \times \underset{\sim}{B}$ instability; the important scale sizes and relevant power spectra would then be determined at early time.

Up to this point, the discussion has focussed on the transverse scale size of frozen barium or nuclear clouds. Here, frozen refers to the property that the plasma cloud is stable to further large-scale structuring by the gradient drift instability. This leads to the second problem: what is the relationship between the frozen transverse scale size and the freezing scale length? The freezing scale length is defined as the scale size at which there is a transition in the power law of the power spectral density (for example, from $\sim k^{-1.5}$ to $\sim k^{-2.5}$). The details of the power spectral density depend not only upon the transverse scale of the cloud or striation, but upon the distribution of transverse scale sizes of striations, as well as the density profiles themselves (i.e., edge effects) (Zabusky et al., 1986; Prettie, 1988). Calculating these quantities is not within the scope of the present 3D model; 3D numerical simulations will be required to better understand many of these issues.

In conclusion, we have presented quantitative estimates of the critical scale size (r_{cr}) of ionospheric plasma striations based on the 3D model developed at NRL (Drake et al., 1988). We have considered parameters typical of both barium clouds and nuclear striations. The relevance of these results to the 'freezing' problem is described as follows. If the initial set of striations has scale sizes such that $r_c > r_{cr}$ then they will be stable to further large-scale structuring because of 3D effects, i.e., they will be 'frozen'. This hypothesis is consistent with barium cloud observations. This leads to the important conclusion that the late time

characteristics of striations (e.g., scale sizes, power spectra, etc.) are determined at early time. Thus, a thorough investigation of early time structuring processes is needed. Applying this idea to the nuclear environment suggests that the structuring of the debris-air shell (being studied experimentally by the NRL laser group), as well as the possible structuring of the deposition region, should be vigorously pursued. Finally, we add that our results are preliminary in the sense that they are based upon an idealized cloud model. To better understand and quantify the nature of 3D effects for realistic clouds requires 3D simulation studies; such studies are currently being conducted at NRL.

ACKNOWLEDGMENTS

We thank Dr. N. Zabusky for helpful discussions. This research has been supported by the Defense Nuclear Agency.

APPENDIX

We present an explicit expression for r_{cr} as a function of the parameters (e.g., M, V_n, T_e, T_i, $\sigma_{||}/\sigma_\perp$, L_z, etc.). Based upon the definition $z_c = (L_z/r_c)(\sigma_\perp/\sigma_{||})^{1/2}$, we rewrite Γ_{c0} (Eq. (9)) as follows

$$\Gamma_{c0} = \begin{cases} \sqrt{2}\,\dfrac{L_z}{r_c}\left(\dfrac{\sigma_\perp}{\sigma_{||}}\right)^{1/2}(M+2)^{-1} & r_c \ll L_z\left(\sigma_\perp/\sigma_{||}\right)^{1/2} \\ \dfrac{3\sqrt{2}}{2}\,\dfrac{L_z}{r_c}\left(\dfrac{\sigma_\perp}{\sigma_{||}}\right)^{1/2}(M+3)^{-1} & r_c = L_z\left(\sigma_\perp/\sigma_{||}\right)^{1/2} \\ \dfrac{ML_z\left(\sigma_\perp/\sigma_{||}\right)^{1/2}}{2r_c/\pi + ML_z\left(\sigma_\perp/\sigma_{||}\right)^{1/2}} & r_c \gg L_z\left(\sigma_\perp/\sigma_{||}\right)^{1/2} \end{cases} \tag{A1}$$

Noting that the critical radius is determined by $\Gamma_0 = \Gamma_{c0}$ we find that r_{cr} is given by

$$r_{cr} = \begin{cases} \sqrt{2}\,\dfrac{V_n}{v_i}\,\dfrac{L_z^2}{\rho_i}\,\dfrac{\sigma_\perp}{\sigma_{||}}(M+2)^{-1} & r_{cr} \ll L_z\left(\sigma_\perp/\sigma_{||}\right)^{1/2} \\ \dfrac{3\sqrt{2}}{2}\,\dfrac{V_n}{v_i}\,\dfrac{L_z^2}{\rho_i}\,\dfrac{\sigma_\perp}{\sigma_{||}}(M+3)^{-1} & r_{cr} = L_z\left(\sigma_\perp/\sigma_{||}\right)^{1/2} \\ \dfrac{\pi}{2}\left(\dfrac{V_n}{v_i}\,\dfrac{L_z^2}{\rho_i}\,\dfrac{\sigma_\perp}{\sigma_{||}} - ML_z\left(\dfrac{\sigma_\perp}{\sigma_{||}}\right)^{1/2}\right) & r_{cr} \gg L_z\left(\sigma_\perp/\sigma_{||}\right)^{1/2} \end{cases} \tag{A2}$$

where $v_i^2 = (T_e + T_i)/m_i$ and $\rho_i = v_i/\Omega_i$.

It is clear from (A2) that r_{cr} is directly proportional to L_z and V_n, and inversely proportional to T_e, T_i, and $\sigma_{||}/\sigma_{\perp}$. The dependence of r_{cr} on M depends upon the value of r_{cr} relative to $L_z(\sigma_{\perp}/\sigma_{||})^{1/2}$. Interestingly, we find that clouds are always stable when $r_c >> L_z(\sigma_{\perp}/\sigma_{||})^{1/2}$ and

$$M > \frac{V_n}{v_i} \frac{L_z}{\rho_i} \left(\frac{\sigma_{\perp}}{\sigma_{||}}\right)^{1/2}. \qquad \text{(A3)}$$

REFERENCES

Drake, J.F., M. Mulbrandon, and J.D. Huba, "Three dimensional equilibrium and stability of ionospheric plasma clouds," to be published in Phys. Fluids, 1988.

Linson, L.M., "Theory of ion cloud dynamics and morphology," Ch. 5 of Analysis of Barium Clouds, RADC-TR-72-336, Vol. 1, Avco Everett Technical Report, 1972.

Prettie, C., "CHECKMATE striations," presentation at Late Time Workshop in Berkeley, 1988.

Sperling, J.L., A.J. Glassman, and C. Chu, "Interim models for the nonlocal specification of freezing wave numbers along the geomagnetic field, JAYCOR Report J200-88-1449/2427, 1988.

Zabusky, N.J., E. Hyman, and M. Mulbrandon, "Projections of plasma cloud structures and their spectra," J. Geophys. Res., 91, 1986.

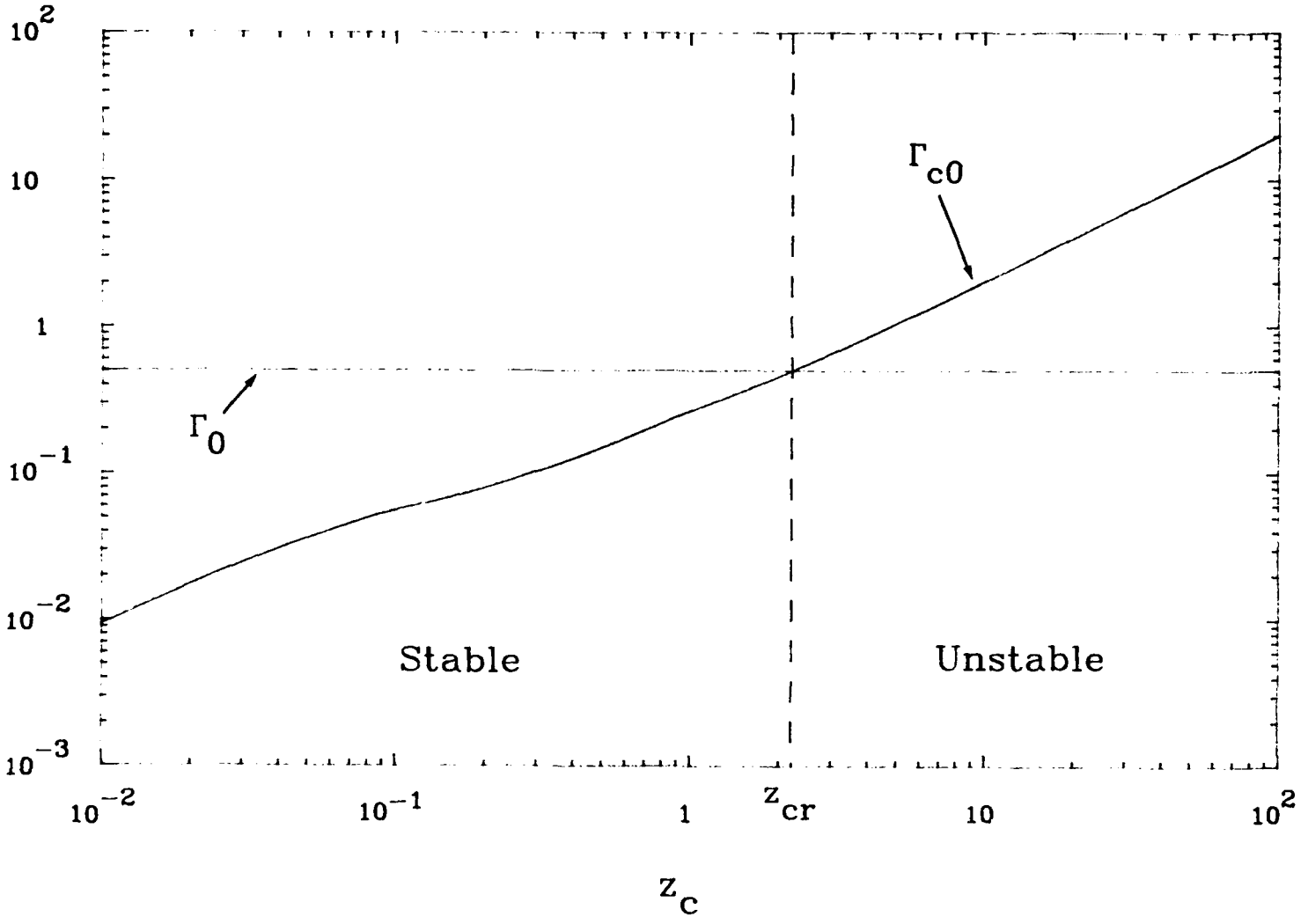

Fig. 1) Plot of Γ_0 and Γ_{c0} vs. z_c for M = 5.0. z_{cr} is determined by the value of z_c for which $\Gamma_0 = \Gamma_{c0}$. Clouds are stable for $\Gamma_0 > \Gamma_{c0}$ (or $z_c < z_{cr}$), and are unstable for $\Gamma_0 < \Gamma_{c0}$ (or $z_c > z_{cr}$) as indicated in the figure.

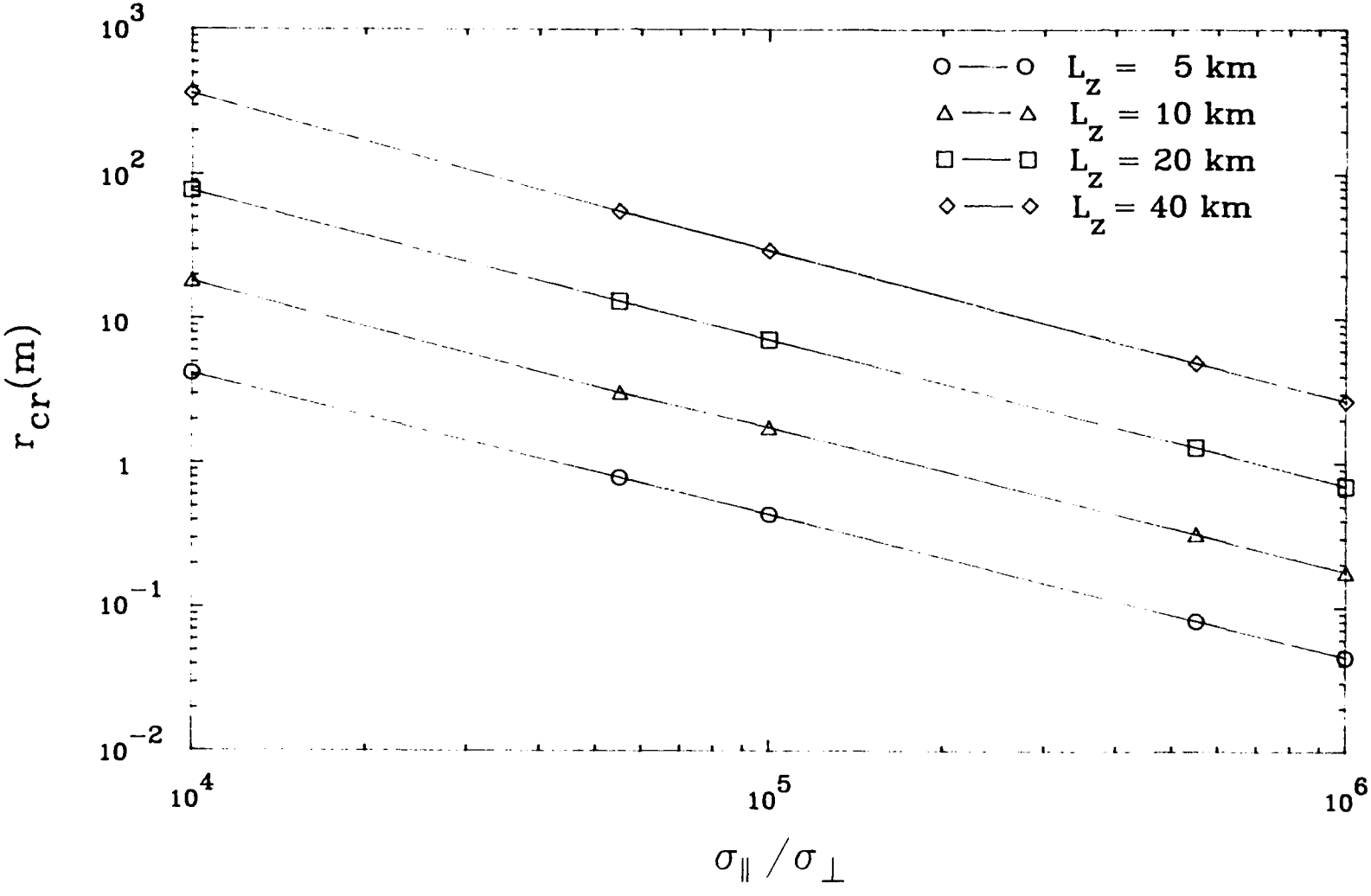

Fig. 2) Plot of r_{cr}(m) vs. $\sigma_{||}/\sigma_{\perp}$ for M = 10, $T_e = T_i$ = 0.1 eV, B = 0.3 G, V_n = 100 m/sec, and L_z = 5 km, 10 km, 20 km, and 40 km. These values are typical of barium clouds released at ~ 180 km.

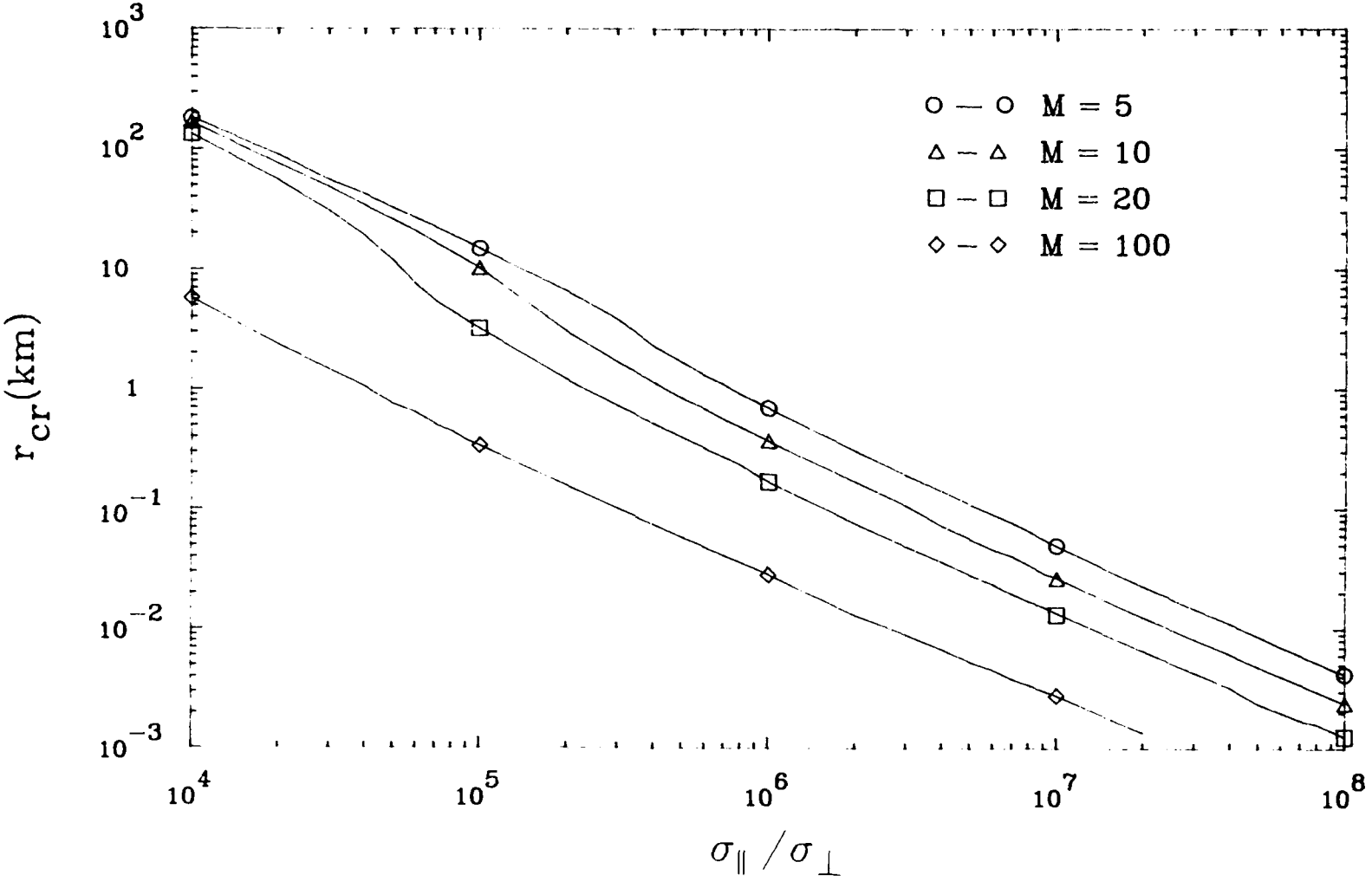

Fig. 3) Plot of r_{cr} (km) vs. $\sigma_{||}/\sigma_{\perp}$ for L_z = 200 km, V_n = 1 km/sec, T_e = T_i = 0.3 eV, and M = 5.0, 10.0, 20.0, and 100.0. These values are representative of a nuclear environment.

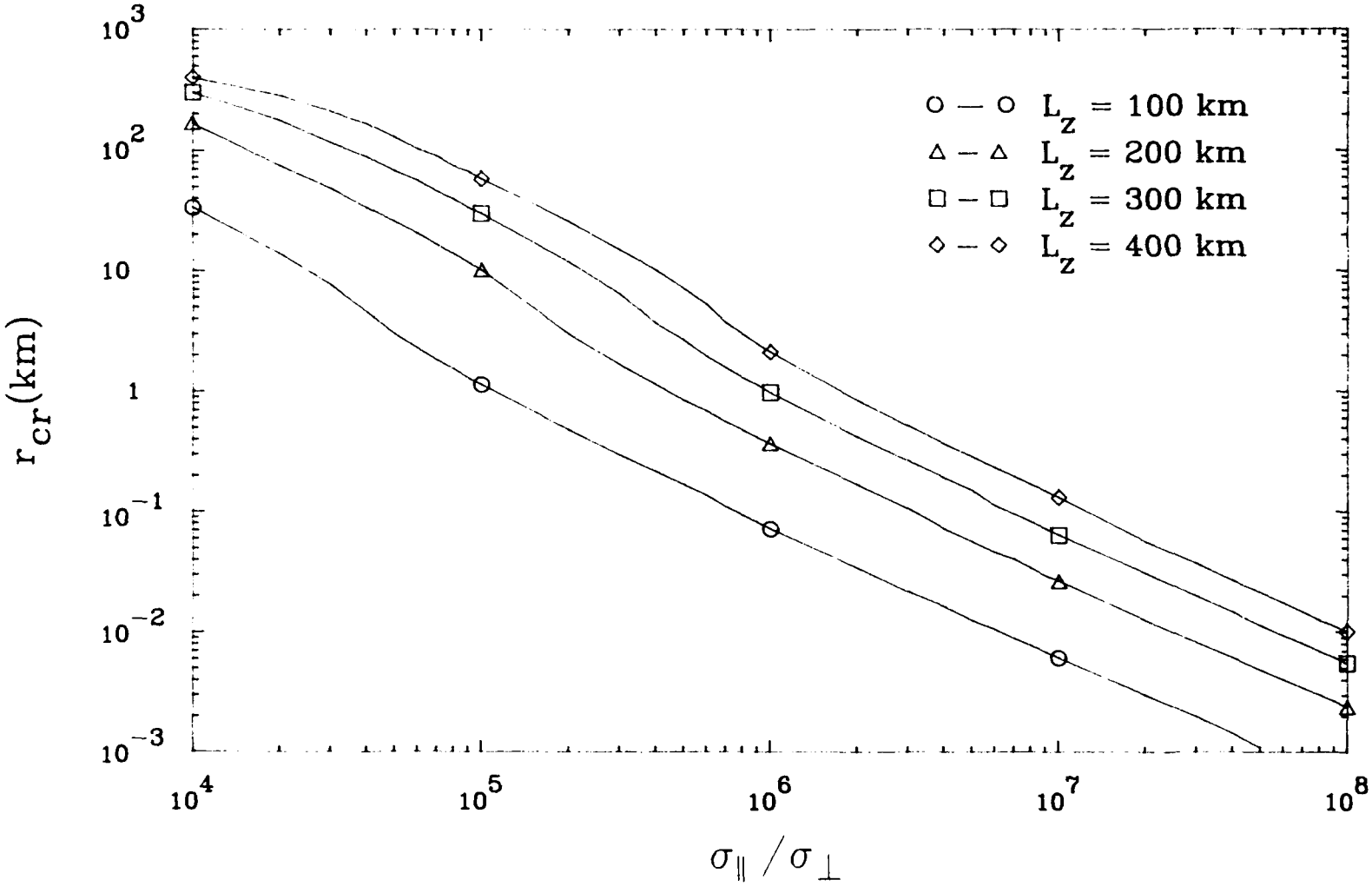

Fig. 4) Plot of r_{cr} (km) vs. $\sigma_{||}/\sigma_{\perp}$ for M = 10, V_n = 1 km/sec, T_e = T_i = 0.3 eV, B = 0.3 G and L_z = 100 km, 200 km, 300 km, and 400 km. These values are representative of a nuclear environment.

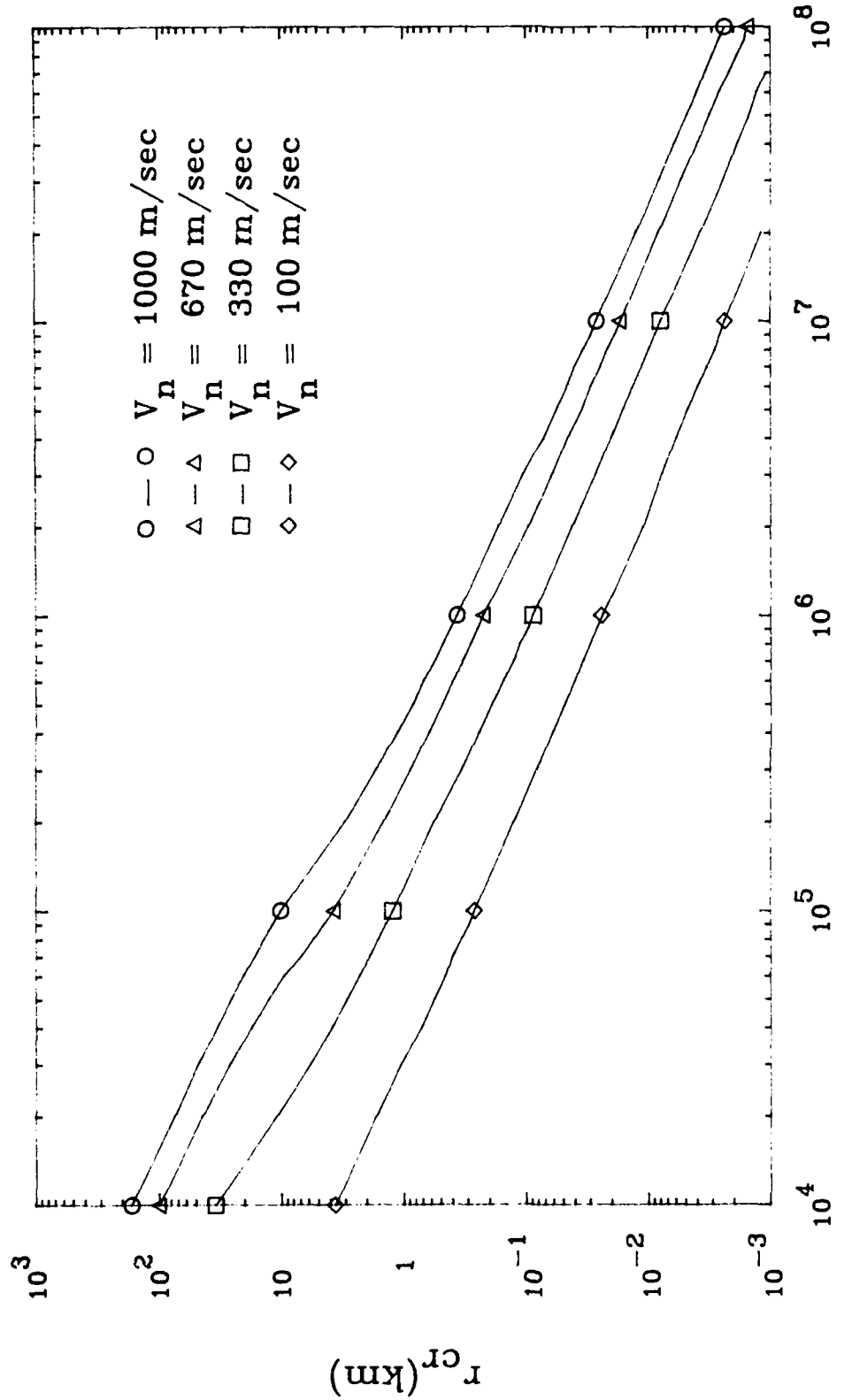

Fig. 5) Plot of r_{cr} (km) vs. $\sigma_{||}/\sigma_{\perp}$ for M = 10, L_z = 200 km, $T_e = T_i$ = 0.3 eV, B = 0.3 G, and V_n = 1000 m/sec, 670 m/sec, 330 m/sec, and 100 m/sec. These values are representative of a nuclear environment.

DISTRIBUTION LIST
(Unclassified Only)

DEPARTMENT OF DEFENSE

ASSISTANT SECRETARY OF DEFENSE
COMM, CMD, CONT 7 INTELL
WASHINGTON, DC 20301

DIRECTOR
COMMAND CONTROL TECHNICAL CENTER
PENTAGON RM BE 685
WASHINGTON, DC 20301
01CY ATTN C-650
01CY ATTN C-312/R. MASON

DIRECTOR
DEFENSE ADVANCED RSCH PROJ AGENCY
ARCHITECT BUILDING
1400 WILSON BLVD.
ARLINGTON, VA 22209
01CY ATTN NUCLEAR MONITORING RESEARCH
01CY ATTN STRATEGIC TECH OFFICE

DEFENSE COMMUNICATION ENGINEER CENTER
1860 WIEHLE AVENUE
RESTON, VA 22090
01CY ATTN CODE R410
01CY ATTN CODE R812

DIRECTOR
DEFENSE NUCLEAR AGENCY
WASHINGTON, DC 20305
01CY ATTN STVL
04CY ATTN TITL
01CY ATTN DDST
03CY ATTN RAAE

COMMANDER
FIELD COMMAND
DEFENSE NUCLEAR AGENCY
KIRTLAND AFB, NM 87115
01CY ATTN FCPR

DEFENSE NUCLEAR AGENCY
SAO/DNA
BUILDING 20676
KIRTLAND AFB, NM 87115
01CY ATTN D. THORNBURG

DIRECTOR
INTERSERVICE NUCLEAR WEAPONS SCHOOL
KIRTLAND AFB, NM 87115
01CY ATTN DOCUMENT CONTROL

JOINT PROGRAM MANAGEMENT OFFICE
WASHINGTON, DC 20330
01CY ATTN J-3 WWMCCS EVALUATION OFFICE

DIRECTOR
JOINT STRAT TGT PLANNING STAFF
OFFUTT AFB
OMAHA, NB 68113
01CY ATTN JSTPS/JLKS
01CY ATTN JPST/G. GOETZ

CHIEF
LIVERMORE DIVISION FLD COMMAND DNA
DEPARTMENT OF DEFENSE
LAWRENCE LIVERMORE LABORATORY
P.O. BOX 808
LIVERMORE, CA 94550
01CY ATTN FCPRL

COMMANDANT
NATO SCHOOL (SHAPE)
APO NEW YORK 09172
01CY ATTN U.S. DOCUMENTS OFFICER

UNDER SECY OF DEFENSE FOR
RESEARCH AND ENGINEERING
DEPARTMENT OF DEFENSE
WASHINGTON, DC 20301
01CY ATTN STRATETIC & SPACE SYSTEMS (OS)

COMMANDER/DIRECTOR
ATMOSPHERIC SCIENCES LABORATORY
U.S. ARMY ELECTRONICS COMMAND
WHITE SANDS MISSILE RANGE, NM 88002
01CY ATTN DELAS-EO/F. NILES

DIRECTOR
BMD ADVANCED TECH CENTER
HUNTSVILLE OFFICE
P.O. BOX 1500
HUNTSVILLE, AL 35807
01CY ATTN ATC-T/MELVIN CAPPS
01CY ATTN ATC-O/W. DAVIES
01CY ATTN ATC-R/DON RUSS

PROGRAM MANAGER
BMD PROGRAM OFFICE
5001 EISENHOWER AVENUE
ALEXANDRIA, VA 22333
01CY ATTN DACS-BMT/J. SHEA

COMMANDER
U.S. ARMY COMM-ELEC ENGINEERING
INSTALLATION AGENCY
FT. HUACHUCA, AZ 85613
01CY ATTN CCC-EMEO/GEORGE LANE

COMMANDER
U.S. ARMY FOREIGN SCIENCE & TECH CTR
220 7TH STREET, N.E.
CHARLOTTESVILLE, VA 22901
01CY ATTN DRXST-SD

COMMANDER
U.S. ARMY MATERIAL DEV & READINESS
COMMAND
5001 EISENHOWER AVENUE
ALEXANDRIA, VA 22333
01CY ATTN DRCLDC/J.A. BENDER

COMMANDER
U.S. ARMY NUCLEAR AND CHEMICAL AGENCY
7500 BACKLICK ROAD
BLDG 2073
SPRINGFIELD, VA 22150
01CY ATTN LIBRARY

DIRECTOR
U.S. ARMY BALLISTIC RESEARCH
LABORATORY
ABERDEEN PROVING GROUND, MD 21005
01CY ATTN TECH LIBRARY/
EDWARD BAICY

COMMANDER
U.S. ARMY SATCOM AGENCY
FT. MONMOUTH, NJ 07703
01CY ATTN DOCUMENT CONTROL

COMMANDER
U.S. ARMY MISSILE INTELLIGENCE AGENCY
REDSTONE ARSENAL, AL 35809
01CY ATTN JIM GAMBLE

DIRECTOR
U.S. ARMY TRADOC SYSTEMS ANALYSIS
ACTIVITY
WHITE SANDS MISSILE RANGE, NM 88002
01CY ATTN ATAA-SA
01CY ATTN TCC/F. PAYAN, JR.
01CY ATTN ATTA-TAC/LTC J. HESSE

COMMANDER
NAVAL ELECTRONIC SYSTEMS COMMAND
WASHINGTON, DC 20360
01CY ATTN NAVALEX 034/T. HUGHES
01CY ATTN PME 117
01CY ATTN PME 117-T
01CY ATTN CODE 5011

COMMANDING OFFICER
NAVAL INTELLIGENCE SUPPORT CENTER
4301 SUITLAND ROAD, BLDG. 5
WASHINGTON, DC 20390
01CY ATTN MR. DUBBIN/STIC 12
01CY ATTN NISC-50
01CY ATTN CODE 5404/J. GALET

COMMANDER
NAVAL OCEAN SYSTEMS CENTER
SAN DIEGO, CA 92152
01CY ATTN J. FERGUSON

NAVAL RESEARCH LABORATORY
WASHINGTON, DC 20375-5000
26CY ATTN CODE 4700/S. OSSAKOW
50CY ATTN CODE 4780/J. HUBA
01CY ATTN CODE 4701
01CY ATTN CODE 7500
01CY ATTN CODE 7550
01CY ATTN CODE 7580
01CY ATTN CODE 7551
01CY ATTN CODE 7555
01CY ATTN CODE 4730/E. MCLEAN
01CY ATTN CODE 4752
01CY ATTN CODE 4730/B. RIPIN
20CY ATTN CODE 2628
01CY ATTN CODE 1004/P. MANGE
01CY ATTN CODE 8344/M. KAPLAN

COMMANDER
NAVAL SPACE SURVEILLANCE SYSTEM
DAHLGREN, VA 22448
01CY ATTN CAPT. J.H. BURTON

OFFICER-IN-CHARGE
NAVAL SURFACE WEAPONS CENTER
WHITE OAK, SILVER SPRING, MD 20910
01CY ATTN CODE F31

DIRECTOR
STRATEGIC SYSTEMS PROJECT OFFICE
DEPARTMENT OF THE NAVY
WASHINGTON, DC 20376
01CY ATTN NSP-2141
01CY ATTN NSSP-2722/
FRED WIMBERLY

COMMANDER
NAVAL SURFACE WEAPONS CENTER
DAHLGREN LABORATORY
DAHLGREN, VA 22448
01CY ATTN CODE DF-14/R. BUTLER

OFFICER OF NAVAL RESEARCH
ARLINGTON, VA 22217
01CY ATTN CODE 465
01CY ATTN CODE 461
01CY ATTN CODE 402
01CY ATTN CODE 420
01CY ATTN CODE 421

COMMANDER
AEROSPACE DEFENSE COMMAND/XPD
DEPARTMENT OF THE AIR FORCE
ENT AFB, CO 80912
01CY ATTN XPDQQ
01CY ATTN XP

AIR FORCE GEOPHYSICS LABORATORY
HANSCOM AFB, MA 01731
01CY ATTN OPR/HAROLD GARDNER
01CY ATTN LKB/
KENNETH S.W. CHAMPION
01CY ATTN OPR/ALVA T. STAIR
01CY ATTN PHD/JURGEN BUCHAU
01CY ATTN PHD/JOHN P. MULLEN

AF WEAPONS LABORATORY
KIRTLAND AFB, NM 87117
01CY ATTN SUL
01CY ATTN CA/ARTHUR H. GUENTHER

AFTAC
PATRICK AFB, FL 32925
01CY ATTN TN

WRIGHT AERONAUTICAL LABORATORIES
WRIGHT-PATTERSON AFB, OH 45433-6543
01CY ATTN AAAI/WADE HUNT
01CY ATTN AAAI/ALLEN JOHNSON

DEPUTY CHIEF OF STAFF
RESEARCH, DEVELOPMENT, AND ACQ
DEPARTMENT OF THE AIR FORCE
WASHINGTON, DC 20330
01CY ATTN AFRDQ

HEADQUARTERS
ELECTRONIC SYSTEMS DIVISION
DEPARTMENT OF THE AIR FORCE
HANSCOM AFB, MA 01731-5000
01CY ATTN J. DEAS
ESD/SCD-4

COMMANDER
FOREIGN TECHNOLOGY DIVISION, AFSC
WRIGHT-PATTERSON AFB, OH 45433
01CY ATTN NICD/LIBRARY
01CY ATTN ETDP/B. BALLARD

COMMANDER
ROME AIR DEVELOPMENT CENTER, AFSC
GRIFFIN AFB, NY 13441
01CY ATTN DOC LIBRARY/TSLD
01CY ATTN OCSE/V. COYNE

STRATEGIC AIR COMMAND/XPFS
OFFUTT AFB, NB 68113
01CY ATTN XPFS

SAMSO/MN
NORTON AFB, CA 02409
(MINUTEMAN)
01CY ATTN MNNL

COMMANDER
ROME AIR DEVELOPMENT CENTER, AFSC
HANSCOM AFB, MA 01731
01CY ATTN EEP/A. LORENTZEN

DEPARTMENT OF ENERGY
LIBRARY, ROOM G-042
WASHINGTON, DC 20545
01CY ATTN DOC CON FOR
A. LABOWITZ

DEPARTMENT OF ENERGY
ALBUQUERQUE OPERATIONS OFFICE
P.O. BOX 5400
ALBUQUERQUE, NM 87115
01CY ATTN DOC CON FOR
D. SHERWOOD

EG&G, INC.
LOS ALAMOS DIVISION
P.O. BOX 809
LOS ALAMOS, NM 85544
01CY ATTN DOC CON FOR
J. BREEDLOVE

UNIVERSITY OF CALIFORNIA
LAWRENCE LIVERMORE LABORATORY
P.O. BOX 808
LIVERMORE, CA 94550
01CY ATTN DOC CON FOR
TECH INFO DEPT
01CY ATTN DOC CON FOR
L-389/R. OTT
01CY ATTN DOC CON FOR
L-31/R. HAGER

LOS ALAMOS NATIONAL LABORATORY
P.O. BOX 1663
LOS ALAMOS, NM 87545
01CY ATTN J. WOLCOTT
01CY ATTN R.F. TASCHEK
01CY ATTN E. JONES
01CY ATTN J. MALIK
01CY ATTN R. JEFFRIES
01CY ATTN J. ZINN
01CY ATTN D. WESTERVELT
01CY ATTN D. SAPPENFIELD

LOS ALAMOS NATIONAL LABORATORY
MS D438
LOS ALAMOS, NM 87545
01CY ATTN S.P. GARY
01CY ATTN J. BOROVSKY

SANDIA LABORATORIES
P.O. BOX 5800
ALBUQUERQUE, NM 87115
01CY ATTN W. BROWN
01CY ATTN A. THORNBROUGH
01CY ATTN T. WRIGHT
01CY ATTN D. DAHLGREN
01CY ATTN 3141
01CY ATTN SPACE PROJ DIV

SANDIA LABORATORIES
LIVERMORE LABORATORY
P.O. BOX 969
LIVERMORE, CA 94550
01CY ATTN B. MURPHEY
01CY ATTN T. COOK

OFFICE OF MILITARY APPLICATION
DEPARTMENT OF ENERGY
WASHINGTON, DC 20545
01CY ATTN DR. YO SONG

NATL. OCEANIC & ATMOSPHERIC
ADMINISTRATION
ENVIRONMENTAL RESEARCH LABS
DEPARTMENT OF COMMERCE
BOULDER, CO 80302
01CY ATTN R. GRUBB

DEPARTMENT OF DEFENSE CONTRACTORS

AEROSPACE CORPORATION
P.O. BOX 92957
LOS ANGELES, CA 90009
01CY ATTN I. GARFUNKEL
01CY ATTN T. SALMI
01CY ATTN V. JOSEPHSON
01CY ATTN S. BOWER
01CY ATTN D. OLSEN

ANALYTICAL SYSTEMS ENGINEERING CORP
5 OLD CONCORD ROAD
BURLINGTON, MA 01803
01CY ATTN RADIO SCIENCES

AUSTIN RESEARCH ASSOCIATION, INC.
1901 RUTLAND DRIVE
AUSTIN, TX 78758
01CY ATTN L. SLOAN
01CY ATTN R. THOMPSON

BERKELEY RESEARCH ASSOCIATES, INC.
P.O. BOX 983
BERKELEY, CA 94701
01CY ATTN J. WORKMAN
01CY ATTN C. PRETTIE
01CY ATTN S. BRECHT

BOEING COMPANY, THE
P.O. BOX 3707
SEATTLE, WA 98124
01CY ATTN G. KEISTER
01CY ATTN D. MURRAY
01CY ATTN G. HALL
01CY ATTN J. KENNEY

CHARLES STARK DRAPER LABORATORY
555 TECHNOLOGY SQUARE
CAMBRIDGE, MA 92139
01CY ATTN D.B. COX
01CY ATTN J.P. GILMORE

COMSAT LABORATORIES
22300 COMSAT DRIVE
CLARKSBURG, MD 20871
01CY ATTN G. HYDE

CORNELL UNIVERSITY
DEPT OF ELECTRICAL ENGINEERING
ITHACA, NY 14850
01CY ATTN D.T. FARLEY, JR.

ELECTROSPACE SYSTEMS, INC.
BOX 1359
RICHARDSON, TX 75080
01CY ATTN H. LOGSTON
01CY ATTN SECURITY/
(PAUL PHILLIPS)

EOS TECHNOLOGIES, INC.
606 WILSHIRE BLVD.
SANTA MONICA, CA 90401
01CY ATTN C.G. GABBARD
01CY ATTN R. LELEVIER

GEOPHYSICAL INSTITUTE
UNIVERSITY OF ALASKA
FAIRBANKS, AK 99701
01CY ATTN SECURITY OFFICER
01CY ATTN T.N. DAVIS
01CY ATTN NEAL BROWN

GTE SYLVANIA, INC.
ELECTRONICS SYSTEMS GRP-
EASTERN DIVISION
77 A STREET
NEEDHAM, MA 02194
01CY ATTN DICK STEINHOF

HSS, INC.
2 ALFRED CIRCLE
BEDFORD, MA 01730
01CY ATTN DONALD HANSEN

ILLINOIS, UNIVERSITY OF
107 COBLE HALL
150 DAVENPORT HOUSE
CHAMPAIGN, IL 61820
01CY ATTN DAN MCCLELLAND
01CY ATTN K. YEH

INSTITUTE FOR DEFENSE ANALYSIS
1801 NO. BEAUREGARD STREET
ALEXANDRIA, VA 22311
01CY ATTN J.M. AEIN
01CY ATTN ERNEST BAUER
01CY ATTN HANS WOLFARD
01CY ATTN JOEL BENGSTON

INTL TELL & TELEGRAPH CORPORATION
500 WASHINGTON AVENUE
NUTLEY, NJ 07110
01CY ATTN TECHNICAL LIBRARY

JAYCOR
P.O. BOX 85154
11011 TORREYANA ROAD
SAN DIEGO, CA 92138
01CY ATTN N.T. GLADD
01CY ATTN J.L. SPERLING

JOHNS HOPKINS UNIVERSITY
APPLIED PHYSICS LABORATORY
JOHNS HOPKINS ROAD
LAUREL, MD 20810
01CY ATTN DOC LIBRARIAN
01CY ATTN THOMAS POTEMRA
01CY ATTN JOHN DASSOULAS

KAMAN SCIENCES CORPORATION
P.O. BOX 7463
COLORADO SPRINGS, CO 80933
01CY ATTN T. MEAGHER

KAMAN TEMPO-CENTER FOR ADVANCED
STUDIES
816 STATE STREET
(P.O. DRAWER QQ)
SANTA BARBARA, CA 93102
01CY ATTN DASIAC
01CY ATTN WARREN S. KNAPP
01CY ATTN WILLIAM MCNAMARA
01CY ATTN B. GAMBILL

LINKABIT CORPORATION
10453 ROSELLE
SAN DIEGO, CA 92121
01CY ATTN IRWIN JACOBS

LOCKHEED MISSILES & SPACE CO., INC
P.O. BOX 504
SUNNYVALE, CA 94088
01CY ATTN DEPT 60-12
01CY ATTN D.R. CHURCHILL

LOCKHEED MISSILES & SPACE CO., INC
3251 HANOVER STREET
PALO ALTO, CA 94304
01CY ATTN MARTIN WALT/
DEPT 52-12
01CY ATTN W.L. IMHOF/
DEPT. 52-12
01CY ATTN RICHARD G. JOHNSON/
DEPT. 52-12
01CY ATTN J.B. CLADIS/
DEPT. 52-12

MARTIN MARIETTA CORPORATION
ORLANDO DIVISION
P.O. BOX 5837
ORLANDO, FL 32805
01CY ATTN R. HEFFNER

MCDONNELL DOUGLAS CORPORATION
5301 BOLSA AVENUE
HUNTINGTON BEACH, CA 02647
01CY ATTN N. HARRIS
01CY ATTN J. MOULE
01CY ATTN GEORGE MROZ
01CY ATTN W. OLSON
01CY ATTN R.W. HALPRIN
01CY ATTN TECHNICAL LIBRARY SERVICES

MISSION RESEARCH CORPORATION
735 STATE STREET
SANTA BARBARA, CA 03101
01CY ATTN P. FISCHER
01CY ATTN W.F. CREVIER
01CY ATTN STEVEN L. GUTSCHE
01CY ATTN R. BOGUSCH
01CY ATTN R. HENDRICK
01CY ATTN RALPH KILB
01CY ATTN DAVE SOWLE
01CY ATTN F. FAJEN
01CY ATTN M. SCHEIBE
01CY ATTN CONRAD L. LONGMIRE
01CY ATTN B. WHITE
01CY ATTN R. STAGAT
01CY ATTN D. KNEPP
01CY ATTN C. RINO

MISSION RESEARCH CORPORATION
1720 RANDOLPH ROAD, S.E.
ALBUQUERQUE, NM 87106
01CY ATTN R. STELLINGWERF
01CY ATTN M. ALME
01CY ATTN L. WRIGHT

MITRE CORPORATION
WESTGATE RESEARCH PARK
1820 DOLLY MADISON BLVD
MCLEAN, VA 22101
01CY ATTN W. HALL
01CY ATTN W. FOSTER

PACIFIC-SIERRA RESEARCH CORP
12340 SANTA MONICA BLVD
LOS ANGELES, CA 90025
01CY ATTN E.C. FIELD, JR

PENNSYLVANIA STATE UNIVERSITY
IONOSPHERE RESEARCH LAB
318 ELECTRICAL ENGINEERING EAST
UNIVERSITY PARK, PA 16802
UNIVERSITY PARK, PA 16802
01 CY ATTN IONOSPHERIC RESEARCH LAB

PHOTOMETRICS, INC.
4 ARROW DRIVE
WOBURN, MA 01801
01CY ATTN IRVING L. KOFSKY

PHYSICAL DYNAMICS, INC.
P.O. BOX 10367
OAKLAND, CA 04610
01CY ATTN A. THOMSON

R & D ASSOCIATES
P.O. BOX 9695
MARINA DEL REY, CA 90291
01CY ATTN FORREST GILMORE
01CY ATTN W.B. WRIGHT, JR
01CY ATTN W.J. KARZAS
01CY ATTN H. ORY
01CY ATTN C. MACDONALD
01CY ATTN BRIAN LAMB
01CY ATTN MORGAN GROVER

RAYTHEON CORPORATION
528 BOSTON POST ROAD
SUDBURY, MA 01776
01CY ATTN BARBARA ADAMS

RIVERSIDE RESEARCH INSTITUTE
330 WEST 42ND STREET
NEW YORK, NY 10036
01CY ATTN VINCE TRAPANI

SCIENCE APPLICATIONS INTERNATIONAL CORPORATION
10260 CAMPUS POINT DRIVE
SAN DIEGO, CA 92121-1522
01CY ATTN L.M. LINSON
01CY ATTN D.A. HAMLIN
01CY ATTN E. FRIEMAN
01CY ATTN E.A. STRAKER
01CY ATTN C.A. SMITH

SCIENCE APPLICATIONS INTERNATIONAL CORPORATION
1710 GOODRIDGE DRIVE
MCLEAN, VA 22102
01CY ATTN J. COCKAYNE
01CY ATTN E. HYMAN

SRI INTERNATIONAL
333 RAVENSWOOD AVENUE
MENLO PARK, CA 94025
01CY ATTN J. CASPER
01CY ATTN DONALD NEILSON
01CY ATTN ALAN BURNS
01CY ATTN G. SMITH
01CY ATTN R. TSUNODA
01CY ATTN D.A. JOHNSON
01CY ATTN W.G. CHESNUT
01CY ATTN C.L. RINO
01CY ATTN WALTER JAYE
01CY ATTN J. VICKREY
01CY ATTN R.L. LEADABRAND
01CY ATTN G. CARPENTER
01CY ATTN G. PRICE
01CY ATTN R. LIVINGSTON
01CY ATTN V. GONZALES
01CY ATTN D. MCDANIEL

TECHNOLOGY INTERNATIONAL CORP
75 WIGGINS AVENUE
BEDFORD, MA 01730
01CY ATTN W.P. BOQUIST

TRW DEFENSE & SPACE SYS GROUP
ONE SPACE PARK
REDONDO BEACH, CA 90278
01CY ATTN R.K. PLEBUCH
01CY ATTN S. ALTSCHULER
01CY ATTN D. DEE
01CY ATTN D. STOCKWELL/
SNTF/1575

VISIDYNE
SOUTH BEDFORD STREET
BURLINGTON, MA 01803
01CY ATTN W. REIDY
01CY ATTN J. CARPENTER
01CY ATTN C. HUMPHREY

UNIVERSITY OF PITTSBURGH
PITTSBURGH, PA 15213
01CY ATTN N. ZABUSKY